A&A 465, 1085–1091 (2007)
DOI: 10.1051/0004-6361:20066616

Astronomy & Astrophysics

Study of the K-H_2 quasi-molecular line satellite in the potassium resonance line

N. F. Allard[1,2], F. Spiegelman[3], and J. F. Kielkopf[4]

[1] Institut d'Astrophysique de Paris, UMR 7095, CNRS, Université Pierre et Marie Curie, 98bis boulevard Arago, 75014 Paris, France
e-mail: allard@iap.fr
[2] Observatoire de Paris-Meudon, LERMA, UMR 8112, CNRS, 92195 Meudon Principal Cedex, France
[3] Laboratoire de Physique Quantique, UMR 5626, CNRS, Université Paul Sabatier, 118 route de Narbonne, 31400 Toulouse, France
[4] Department of Physics and Astronomy, University of Louisville, Louisville, KY, 40292, USA

Received 21 October 2006 / Accepted 20 December 2006

ABSTRACT

Context. The optical spectra of L and T-type dwarfs exhibit a continuum dominated by the far wings of the absorption profiles of the Na 3s–3p and K 4s–4p doublet perturbed by molecular hydrogen and helium. The presence of a broad absorption feature in the blue wing of the K 4s–4p doublet may be attributed to the K-H_2 quasi-molecular line satellite as we predicted in a previous work.
Aims. The position of the predicted line satellite was not in good agreement with the observed feature. This was a motivation to compute new interaction potentials and corresponding profiles.
Methods. New molecular potentials for K-H_2 were computed using a valence pseudopotential with Gaussian orbitals on potassium, for an H_2 molecule assumed to be in its ground state. A quasi-full three-electron multireference calculation agrees very well with available spectroscopic data. The potentials and radiative dipole transition moments were input data for a unified spectral line shape evaluation of the complete K resonance line profile.
Results. We show that these improved potentials now predict a line satellite at the position that is observed in late brown dwarf spectra. The existence, shape and strength of this feature is found to depend strongly on temperature, as well on the abundance ratio of potassium and sodium.
Conclusions. The structure of the continuum in brown dwarf spectra from 500 to 1000 nm is determined by radiative collisions of alkali atoms with H_2 molecules. We conclude that the sensitivity of the spectrum to temperature, pressure and abundances is a tool for determining basic parameters of brown dwarf atmospheres, provided that the physics underlying its formation is described well.

Key words. line: profiles – radiation mechanisms: general – stars: atmospheres

1. Introduction

The importance of the far wings of the potassium doublet, centered at 768 nm in the spectra of methane brown dwarfs, has been demonstrated by Burrows et al. (2000). They concluded "that the neutral alkali metals play a central role in the near-infrared and optical spectra of methane dwarfs and that their lines have the potential to provide crucial diagnostics of brown dwarfs properties".

The studies of observed L and T dwarfs by Liebert et al. (2000) and Burrows et al. (2001) showed clearly the importance of extended wings of both sodium and potassium doublets. They pointed out the need for more accurate line profile calculations. Simple treatment such as Lorentzian profiles coming from impact broadening theory is only valid in the core of the line and cannot be used to describe the line wing. Cutoffs of the line wings of Lorentzian profiles have been introduced by Burrows et al. (2000), Allard et al. (2001), Tsuji et al. (1999), Marley et al. (2002), Saumon et al. (2000), Geballe et al. (2001) to try to fit observations.

A major improvement was made by Burrows & Volobuyev (2003) using multiconfiguration self-consistent field Hartree-Fock potentials in the Szudy & Baylis (1975, 1996) line shape theory. The cutoffs of the wings physically come from the Boltzmann factor in the expression of the Unified Franck-Condon profile.

In Allard et al. (2003) we presented absorption profiles of sodium and potassium perturbed by He and H_2 calculated in a unified line shape semi-classical theory (Allard et al. 1999) using molecular potentials of Pascale (1983) to describe the alkali-He interaction and those of Rossi & Pascale (1985, hereafter RP85) for the alkali-H_2 interaction. This work was extended to the case of Li-He/H_2 collisional line profiles (Allard et al. 2005). These calculations used Hund's case *a* and *b* for determining the shape of spectral line and neglected the fine structure that was insignificant in the far wing.

Similar profiles in the line wings were obtained for light alkalis perturbed by helium by Zhu et al. (2005, 2006) in full quantum mechanical calculations in the binary approximation. They used Na-He and K-He interaction potentials computed respectively by Theodorakopoulos & Petsalakis (1993) and by Santra & Kirby (2005, hereafter SK05).

Our line profiles calculated with the unified theory were included as a source of opacity in model atmospheres and synthetic

spectra using the Allard et al. (2001) stellar atmosphere program PHOENIX. This treatment has improved the comparison of synthetic spectra of brown dwarfs with observations (Allard et al. 2003; Johnas et al. 2006).

Blue satellites are predicted in the far wing of alkali-He/H_2 line profiles. Such satellite bands of alkali metals perturbed by rare gas have been extensively studied in the past (Allard & Kielkopf 1982, and references therein). The K-H_2 quasi-molecular satellite appears on the synthetic spectrum presented in Fig. 4 of Allard et al. (2003). This feature might have been observed in brown dwarf spectra (Allard et al. 2006a,b). However, its theoretical position does not correspond exactly to the *observed* one which was identified in T dwarfs by Burgasser et al. (2003) as the CaH system. According to Allard et al. (2006a,b) the CaH band does not seem to match the observed feature and the K-H_2 satellite would be the most natural explanation.

If such satellites could be detected, they could serve as a diagnostic of temperature in the brown dwarf atmosphere, much in the way that the H-H and H-H^+ satellites on Lyman series lines are temperature diagnostics in white dwarf spectra (Allard et al. 2004, and references therein). The interactions of an alkali atom with H_2 depend on the orientation of the H_2 axis relative to the collision axis. As a consequence, a useful theoretical spectrum will need potentials as a function of H_2 orientation (with respect to the interaction axis) as well as a function of the alkali-H_2 separation. In the work of RP85, the alkali-H_2 molecular potentials were calculated using model potentials completed by polarization operators, for the two symmetries C_{2v} ($\Theta = 90°$) and $C_{\infty v}$ ($\Theta = 0$), where Θ is the angle between the direction of the molecular axis and the interaction axis. In these calculations, the alkali-H_2 complex was considered as a system with a single active electron.

Ab initio calculations of the potentials of K-H_2 (together with K-He) have been reported by SK05. In their all-electron calculation, the states were determined from a MRPT2 variational/perturbative Configuration Interaction scheme including the 4s and 4p shells, and also single and double excitations from the 3s and 3p shell accounting for core-valence polarization and correlation. From their potentials, a K-H_2 satellite can be predicted in the region ranging from about 685 nm in symmetry $C_{\infty v}$ to 692 nm in C_{2v} symmetry.

In the present work, we describe new calculations of the potential energy surfaces in which the two electrons of H_2 and the valence electron of K are explicit, the latter atom being described by a valence pseudopotential complemented by a core-polarization type pseudopotential (CPP) to account for polarization and core polarization effects following Müller et al. (1984a,b). Such a methodology was found to produce results with high accuracy in various systems, including alkali diatomics, K_2 (Magnier et al. 1996, 2004), and metal-rare gas systems (El Hadj Ben Rhouma et al. 2002; Spiegelman et al. 2002) including potassium. We present theoretical calculations of the unified line profile of this alkali perturbed by molecular hydrogen with an emphasis on properties of the line satellite. The satellite's position is shown to be in agreement with one of the features observed in brown dwarf spectra. This spectral region, from 680 to 740 nm, is very temperature dependent and is very constraining in the comparison of atmosphere models with observation because of the overlap of the red wing of the (3s–3p) resonance line of sodium with the blue wing of the (4s–4p) resonance line of potassium.

2. New molecular potentials and resulting profiles

2.1. K-H_2 diatomic potentials without spin-orbit coupling

The valence pseudopotential used on potassium was developed by Durand & Barthelat (1975) and Jeung et al. (1982). In the present calculations, the Gaussian type orbital (GTO) basis set on potassium was 7s6p4d, including very diffuse Gaussian functions (the smallest exponents are $\zeta = 0.0016$, 0.0018 and 0.003 for s, p and d type GTO, respectively). The dipole core polarisability of potassium K^+ was taken as $\alpha = 5.354\ a_0^3$, and a step-like cut-off function with $\rho = 2.067\ a_0$ was used for the electric field (Foucrault et al. 1992) in the CPP operator $-\frac{1}{2}\alpha E^2$ on potassium. This provides a 4s–4p transition energy $\nu_{4s4p} = 13\,047\ \mathrm{cm}^{-1}$ to be compared with the all-electron value $\nu_{at} = 12\,290\ \mathrm{cm}^{-1}$ of SK05 and $\nu_{4s4p} = 13\,023\ \mathrm{cm}^{-1}$ experimentally. The transition dipole moment is found to be 3.03 ea_0, versus 2.92 ea_0 experimentally, to be compared with 3.10 ea_0 in the all-electron calculation of SK05.

A 7s5p6d GTO basis set was used on hydrogen centers. With this basis set and a 2-electron Full Configuration Interaction (FCI) calculation, the spectroscopic data of the $X^1\Sigma^+$ ground state of KH are $D_e = 14\,651\ \mathrm{cm}^{-1}$, $r_e = 4.20\ a_0$, with the experimental data $D_e = 14\,772.7\ \mathrm{cm}^{-1}$, $r_e = 4.233\ a_0$. Those of the $A^1\Sigma^+$ state are $T_e = 18\,981\ \mathrm{cm}^{-1}$, $D_e = 8696\ \mathrm{cm}^{-1}$, $r_e = 7.07\ a_0$, $\omega_e = 220\ \mathrm{cm}^{-1}$ to be compared with the experimental data $T_e = 19\,059\ \mathrm{cm}^{-1}$, $D_e = 8736\ \mathrm{cm}^{-1}$, $r_e = 7.110\ a_0$ (Stwalley et al. 1991; Rafi et al. 1996; Camacho et al. 1998).

The molecule H_2 is assumed to be in its ground state. In the present basis set, its FCI dissociation energy is $D_e = 38\,119\ \mathrm{cm}^{-1}$ at an equilibrium distance $r_e = 1.40\ a_0$ (the converged theoretical value for D_e is $38\,292.8\ \mathrm{cm}^{-1}$, Kolos & Wolniewicz 1968). In the case of the KH_2 complex, a quasi-full three-electron Configuration Interaction (CI) was achieved using the multireference MRPT2 Toulouse package CIPSI (Huron et al. 1973). All determinants having a contribution in the first-order wavefunction larger than $\tau = 10^{-5}$ with respect to a main reference subspace were generated and involved in a variational CI. The main reference space itself included all single excitations with respect to the ground state configuration, ensuring that all triples (actually the full CI space) entered the selection. It was checked that the total energy contribution of the rest was less than $10\ \mathrm{cm}^{-1}$. Spin-orbit (SO) coupling is rather small for potassium ($\zeta_{4p} = 54\ \mathrm{cm}^{-1}$). Its effect is dominant close to the line center and not essential in the wings. It was not included here to allow direct comparison with the profiles of Allard et al. (2003).

The calculations were carried out for the $C_{\infty v}$ (linear) symmetry group, the C_{2v} (T-shape) symmetry group, and C_s geometries ($\Theta = 30$, 45 and 60°) over a wide range of distances R between the K atom and the center-of-mass of the molecule H_2, the geometry of H_2 being fixed at the equilibrium value $r_e = 1.40$ au.

In $C_{\infty v}$ symmetry ($\Theta = 0°$), the ground state X has $^2\Sigma^+$ symmetry, while the 4p excited configuration generates one two-fold $^2\Pi$ state (labeled A, with attractive character) and one essentially repulsive $^2\Sigma^+$ state. In the C_s symmetry group, the $^2\Pi$ state splits into $2A'$ and $2A''$ components, the X and the $^2\Sigma^+$ being correlated with the $^2A'$ manifold. In C_{2v} symmetry ($\Theta = 90°$), the ground state belongs to the $^2A_1$ manifold, the excited states to the $^2B_1$ and $^2B_2$ and $^2A_1$ manifolds respectively, in increasing energetic order.

Figures 1 and 2 present the potential energy surfaces $V_e[R(t)] = E_e[R(t)] - E_e^\infty$ in the $C_{\infty v}$ and the C_{2v} symmetries, respectively. The other results in C_s geometries ($\Theta = 30$, 45 and 60°) range between those two limits. The major difference

Table 1. Dependence of the position of the line satellite on the computed K-H_2 potential.

Symmetry	$\Delta\omega$ (cm^{-1}) SK05	λ (nm) SK05	R_{ext}(Å)	$\Delta\omega$ (cm^{-1}) S06	λ (nm) S06	R_{ext} (Å)	$\Delta\omega$ (cm^{-1}) RP85	λ (nm) RP85	R_{ext} (Å)
$C_{\infty v}$		685[a]	3.06	1617	683[a]	3	207	662.5[a]	3.1
				1415	692[b]		1912	669.5[b]	
C_{2v}		692[a]	3.23	1450	690.6[a]	3.16	1700	679.2[a]	3.37
				1302	698[b]		1572	685.1[b]	

[a] Predicted. [b] Line profile.

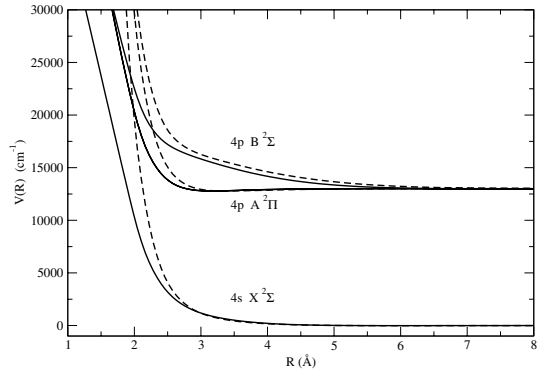

Fig. 1. Potential curves for the X, A and B states of the K-H_2 molecule without spin-orbit coupling for the $C_{\infty v}$ symmetry of S06 compared to RP85 (dashed curves).

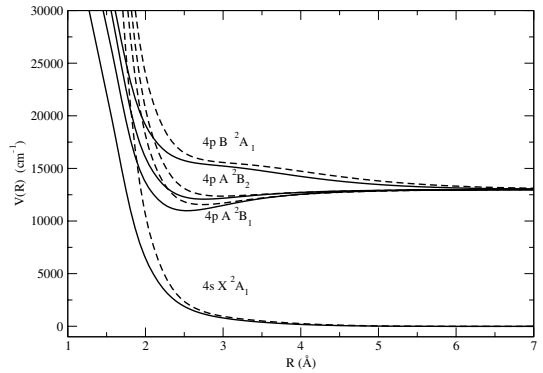

Fig. 2. K-H_2 potentials for the resonance lines for the C_{2v} symmetry without spin-orbit coupling of S06 compared to RP85 (dashed curves).

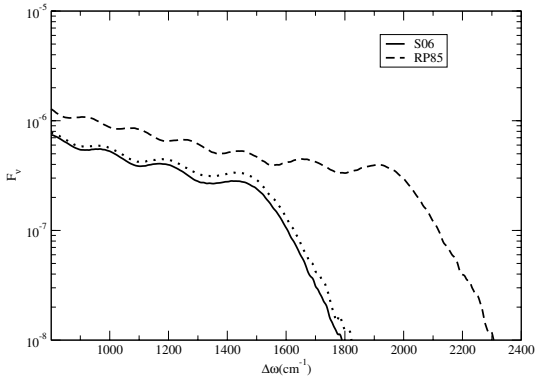

Fig. 3. Blue wing of K-H_2 collisional profiles in ΔV units for the symmetry $C_{\infty v}$ using S06 and RP85 potentials. The dotted line indicates the profile using S06 potentials but in the constant dipole moment approximation (T = 1000 K, $n_{H_2} = 1 \times 10^{19}$ cm^{-3}).

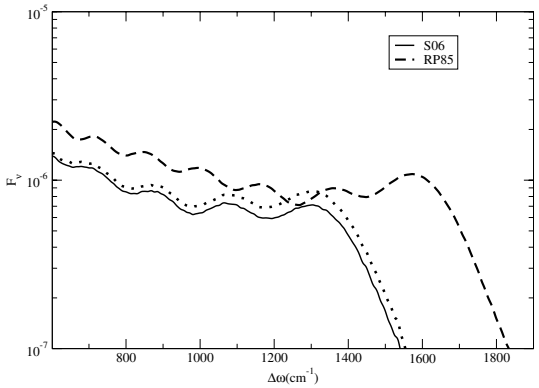

Fig. 4. Blue wing of K-H_2 collisional profiles in ΔV units for the symmetry C_{2v} using S06 and RP85 potentials. The dotted line indicates the profile using S06 potentials but in the constant dipole moment approximation (T = 1000 K, $n_{H_2} = 1 \times 10^{19}$ cm^{-3}).

with respect to RP85 is that our potentials are systematically less repulsive than theirs, the state mostly affected being state B which starts to deviate from RP85 as soon as $R < 5$ Å when decreasing the separation. This might be attributed either to a too repulsive component in the model potential of RP85, or to a too repulsive character of the short range K-H_2^+ core-core contribution that must be added to the single electron energy in the model potential scheme, or both. In the present calculation, as in that of SK05, the latter contribution is explicitly calculated. This difference in the B state will strongly affect the blue satellite position.

2.2. Study of the position of the K-H_2 line satellite

Blue satellite bands in alkali-He/H_2 profiles are correlated with maxima in the excited B state potentials and can be predicted from the maxima in the difference potentials ΔV for the B-X transition (Allard et al. 2003, 2005, 2006; Zhu et al. 2005, 2006). In the following we will restrict our study to the B-X transition as we focus on the K-H_2 satellite. Details of the calculations of the other transitions are presented in Spiegelman (2006, hereafter S06).

The difference potential, $\Delta V(R)$, is given by

$$\Delta V(R) \equiv V_{e'e}[R(t)] = V_{e'}[R(t)] - V_e[R(t)], \quad (1)$$

and represents the difference between the electronic energies of the quasimolecular B-X transition.

The line profiles have been calculated at T = 1000 K for a fixed molecular hydrogen density ($n_{H_2} = 1 \times 10^{19}$ cm^{-3}). They are presented in Figs. 3 and 4. We notice in Fig. 3 the satellite at 1415 cm^{-1} for S06 and at 1875 cm^{-1} for RP85. They correspond respectively to ΔV = 1620 and 2070 cm^{-1} in Fig. 6. Their positions depend on the value of the extrema of the potential difference $\Delta V(R)$, but they are always closer to the line center than

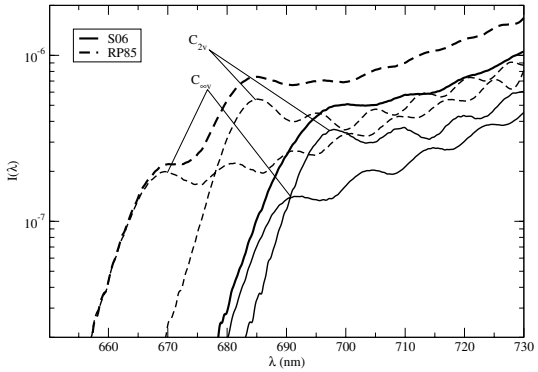

Fig. 5. Total line profile compared to the contributions of the $C_{\infty v}$ and C_{2v} symmetries. (T = 1000 K, $n_{H_2} = 1 \times 10^{19}$ cm^{-3}).

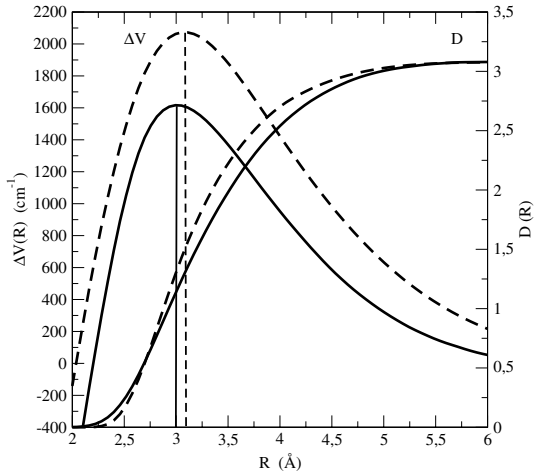

Fig. 6. ΔV and modulated dipole at 1000 K for the symmetry $C_{\infty v}$. S06 (full line), RP85 (dashed line).

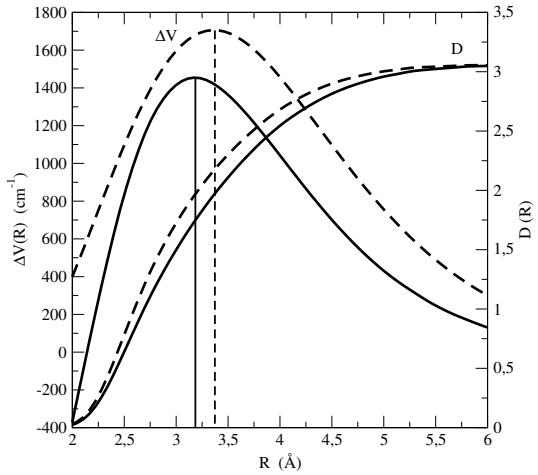

Fig. 7. ΔV and modulated dipole at 1000 K for the symmetry C_{2v}. S06 (full line), RP85 (dashed line).

this value. The contribution of the K-H_2 potentials for the other symmetry gives satellites at 1300 cm^{-1} for S06 and at 1570 cm^{-1} for RP85 (Fig. 4). We have summarized these values in Table 1 and compared them to what can be expected from the potentials of SK05. The predictions that a K-H_2 satellite would appear from about 685 nm for the symmetry $C_{\infty v}$ to 692 nm for the

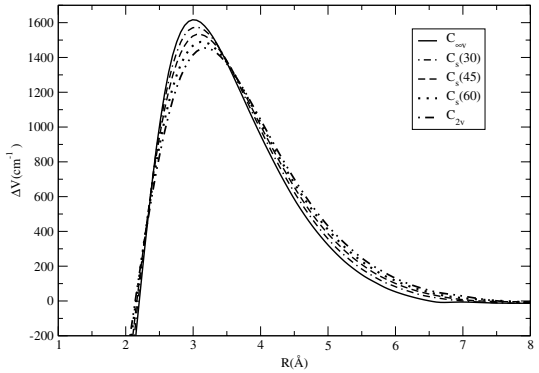

Fig. 8. ΔV for the various geometries, namely C_{2v}, $C_s(60°)$, $C_s(45°)$, $C_s(30°)$ and $C_{\infty v}$.

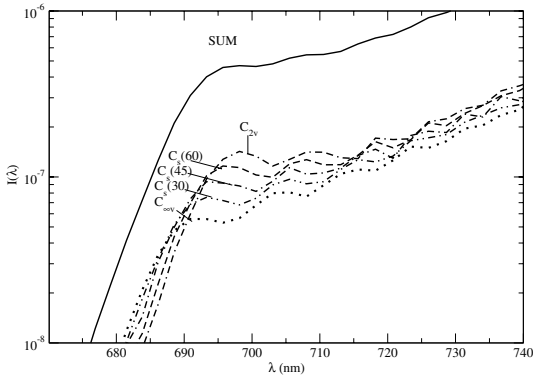

Fig. 9. Contribution of the various geometries, C_{2v}, $C_s(60°)$, $C_s(45°)$, $C_s(30°)$ and $C_{\infty v}$ to the K-H_2 satellite.

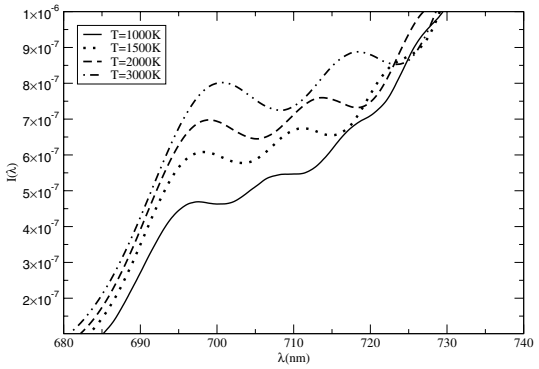

Fig. 10. Variation of the strength of the K-H_2 satellite with temperatures for a fixed molecular hydrogen density (1×10^{19} cm^{-3}).

symmetry C_{2v} would lead to a line satellite at the same position as the observed broad absorption.

The two calculated orientation angles of H_2 shown in Fig. 5 give satellites which appear as two bumps on the RP85 total profile, whereas they are smeared out on the S06 total profile and lead just to a rapidly decreasing wing beyond the position of the satellite band. Taking all the orientations into account should lead to a broad band with an extension of about 10 nm.

2.3. Angular dependence of ΔV for the B-X transition

In the new S06 potentials we also have investigated the dependence of the interaction potentials on other angles Θ between the H_2 axis and the line connecting the K atom with the

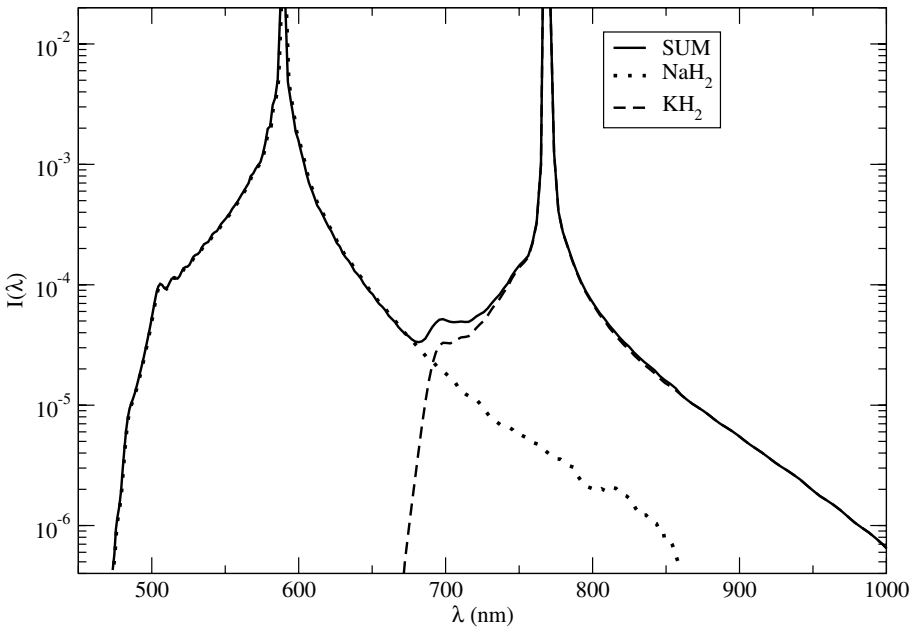

Fig. 11. Sum of Na and K alkali profiles perturbed by molecular hydrogen, weighted by their line strength at solar abundance compared to the contribution of Na and K for a fixed molecular hydrogen density (1×10^{19} cm^{-3}), T = 1500 K.

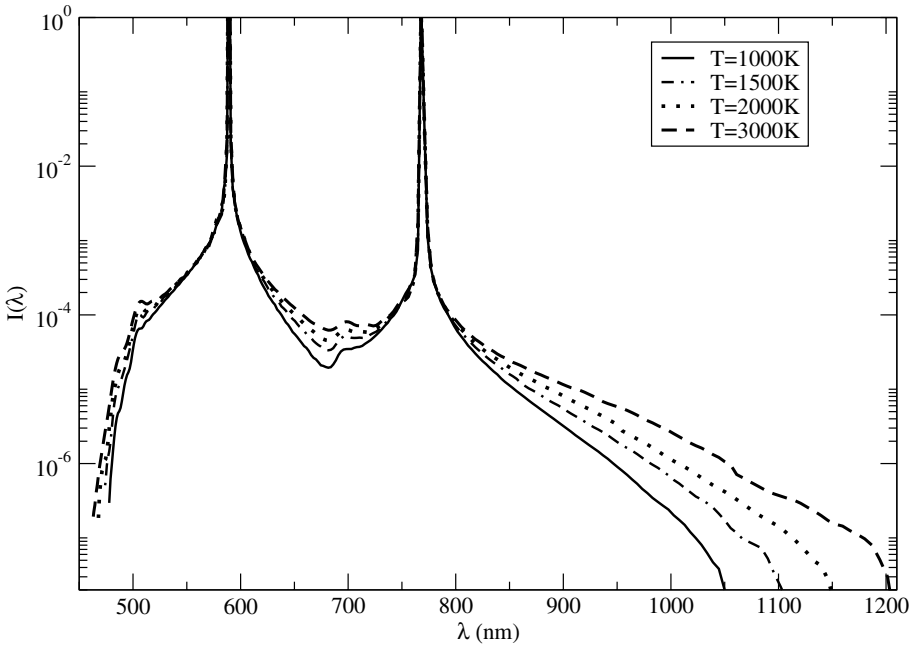

Fig. 12. Sum of Na and K alkali profiles perturbed by molecular hydrogen, weighted by their solar abundance. Four different temperatures are compared for a fixed molecular hydrogen density (1×10^{19} cm^{-3}).

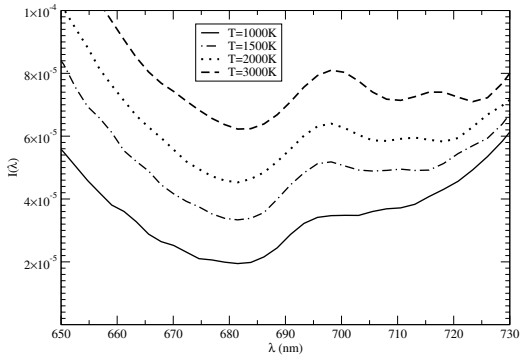

Fig. 13. Close-up of the K-H_2 satellite for different temperatures for a fixed molecular hydrogen density (1×10^{19} cm^{-3}).

center-of-mass of the molecule H_2. In Fig. 8 we plot ΔV for different orientations of the H_2 molecule.

The corresponding profiles are displayed in Fig. 9 compared to the total profile after averaging over the different angles. As a first step we assume an equal weight for each orientation to calculate the sum shown in Fig. 9.

3. Radiative dipole transition moments

While the position of the line satellites critically depends on the interaction potential, their amplitude depends on both the interaction potential and the radiative dipole moments. In Allard et al. (2003) we were limited by a lack of knowledge of the dependence of the radiative transition dipole moment on R for each molecular state. For the alkali-H_2 systems, the dipole moments were assumed to remain constant throughout the collision and equal to their asymptotic value.

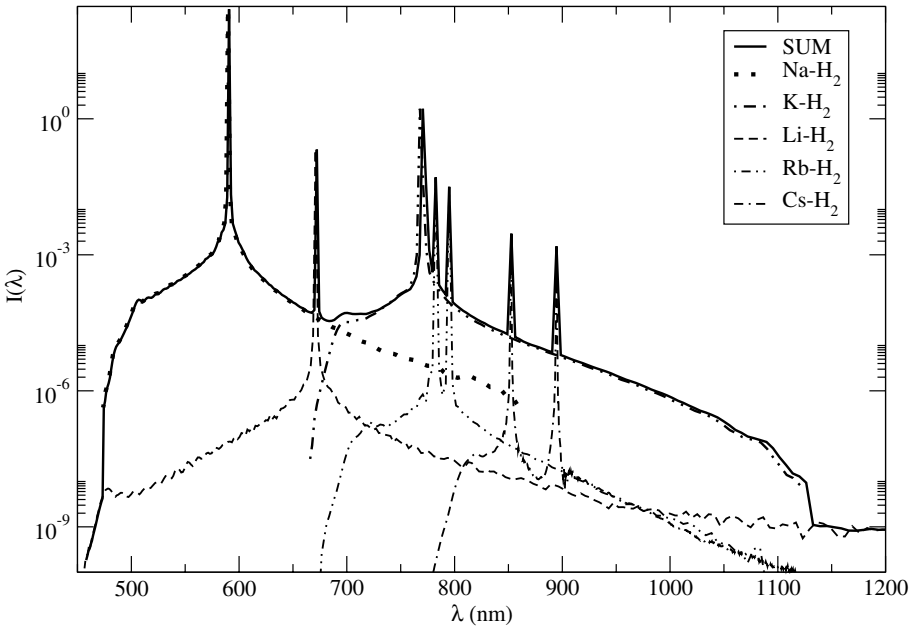

Fig. 14. Sum of the alkali profiles perturbed by molecular hydrogen, weighted by their solar abundance at $T = 1500$ K. compared to the sum restricted to sodium and potassium for a fixed molecular hydrogen density (1×10^{19} cm^{-3}). The Li-H2 total profile also is overplotted.

3.1. Calculations of dipole moments

The transition dipole moments have been computed by SK05 and S06. They both find that the dipole moment decreases with decreasing R.

3.2. Influence of dipole moment on the amplitude of the line satellite

For a transition $\alpha = (i, f)$ from initial state i to final state f, we define $\tilde{d}_{ee'}(R(t))$ as a *modulated* dipole (Allard et al. 1999)

$$D(R) \equiv \tilde{d}_{ee'}[R(t)] = d_{ee'}[R(t)]e^{-\frac{\beta}{2}V_e[R(t)]}, \quad (2)$$

where β is the inverse temperature $(1/kT)$. Here V_e is the ground state potential as we consider absorption profiles.

In Figs. 3 and 4 we have compared the blue line wings in the region of the K-H_2 satellite obtained with constant and variable dipoles. The effect on the satellite amplitude is not very significant. Our calculations, within the assumption of constant dipole moment, were a good first approximation.

The different shape of the wings and the loss of contrast of the line satellite come from the lower value of R_m, the internuclear separation at which the difference potential is a maximum, the line satellite being predominantly due to perturbers at this distance. The average number of perturbers in the interaction volume at R_m is the determining parameter for the amplitude of the satellites on the spectral line (Allard 1978; Royer 1978). It will decrease as R_m^2.

The satellite amplitude also depends on the value of the electric dipole transition moment in the internuclear region where the line satellite is formed (Allard et al. 1998). Because of a lower R_m and a fast variation with R of the *modulated* dipole moment, the amplitude of the resulting satellite decreases. The modulated dipole moment can be seen in Figs. 6 and 7 where we display $D(R)$ together with the corresponding $\Delta V(R)$. Although the line satellite now has a position in agreement with observations, the new potentials lead to less contrast of the satellite. It may even seem to have disappeared at the lowest temperatures.

4. Importance of temperature and metallicity dependence on the K-H_2 satellite

Line satellite features in wings of the spectral line formed by transitions between quasi-molecular states during atomic collisions are temperature dependent through the Boltzmann factor which modulates the dipole moment. In Fig. 10 we plot the appearance of the K-H_2 satellite at temperatures of astrophysical interest. This line satellite is far removed to the blue from the KI resonance line center, and is actually closer to the LiI line. It is therefore necessary to take into proper account the total contribution of both K, Li and Na perturbed by H_2 and to study the dependence of this part of the complete wing upon temperature.

4.1. Sum of the alkali profiles perturbed by H_2

The abundance of Na is expected to be the highest among the alkali metals, and the red wing of the Na-H_2 profile is dominant in the spectrum. The total profile resulting from both Na and K perturbed by collisions with molecular hydrogen is shown in Fig. 12. We notice that the K-H_2 satellite is still apparent. It is even more prominent because the overlap of the two wings leads to an enhancement in its contrast compared to the line wing of K alone. Figure 13 shows a close-up of the 650–730 nm spectral region to illustrate this effect at different temperatures.

We show the sum of the alkali profiles in Fig. 14, done according to Eq. (51) of Allard et al. (1999). Each alkali profile is weighted by its line strength. A detailed study of theoretical line profile calculations of the heavier alkalis perturbed by helium and molecular hydrogen is described in Allard & Spiegelman (2006). To illustrate clearly the relative importance of the different alkali resonance lines through this region, we multiplied each profile by the solar abundance of the alkali to produce the sum shown in Fig. 14. We can see the contribution of each alkali species in the region from 450 to 1200 nm. For λ below 474 nm, only the Li-H_2 profile contributes. The rapid decrease below 500 nm is due to the Na-H_2 satellite whereas the contribution of the K-H_2 profile stops above 1120 nm.

As we see here, and as Burrows et al. (2002) point out, the absorption by the sodium line is a natural explanation for the suppression of flux shortward of 700 nm in L-type and T-type

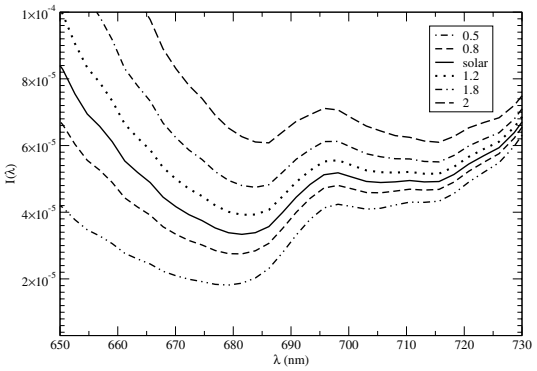

Fig. 15. Variation of the strength of the K-H_2 satellite with the Na abundance, the K abundance remains the solar one. (Calculations are done for a fixed molecular hydrogen density (1×10^{19} cm^{-3}) and for T = 1500 K.

dwarf spectra. Burrows et al. (2002) showed that the T-dwarf spectral types are not determined solely by $T_{\rm eff}$ and they suggested that gravity and, perhaps, metallicity also play a role. Here we see clearly how the different alkalis contribute to determine the spectrum in this region.

4.2. Influence of metallicity

To study the influence of the overlap of the blue wing of Na-H_2 on the strength of the K-H_2 satellite we have allowed the abundance of Na to vary from 0.5 solar abundance to 2 solar abundance. Figure 15 shows the sensitivity of this region of the spectrum with the variation with sodium abundance. The K-H_2 satellite appearance is then very sensitive to both the abundance and the temperature and may be used as a temperature diagnostic.

The next step will be to include these new profiles in the model atmospheres and synthetic spectra of brown dwarfs.

References

Allard, F., Hauschildt, P. H., Alexander, D. R., Tamanai, A., & Schweitzer, A. 2001, ApJ, 556, 357

Allard, F., Allard, N. F., & Spiegelman, F. 2006a, Conference SF2A, 26–30 June 2006, Paris

Allard, F., Allard, N. F., Johnas, C. M. S., et al. 2006b, IAU XXVIth Assembly, 14–25 August 2006, Prague

Allard, N. F. 1978, J. Phys. B.: At. Mol. Opt. Phys., 11, 1383

Allard, N. F., & Kielkopf, J. F. 1982, Rev. Mod. Phys., 54, 1103

Allard, N. F., & Spiegelman, F. 2006, A&A, 452, 351

Allard, N. F., Royer, A., Kielkopf, J. F., & Feautrier, N. 1999, Phys. Rev. A, 60, 1021

Allard, N. F., Allard, F., Hauschildt, P. H., Kielkopf, J. F., & Machin, L. 2003, A&A, 411, L473

Allard, N. F., Kielkopf, J. F., & Loeillet, B. 2004, A&A, 424, 347

Allard, N. F., Allard, F., & Kielkopf, J. F. 2005, A&A, 440, 1195

Burgasser, A. J., Kirkpatrick, J. D., Liebert, J., & Burrows, A. 2003, ApJ, 594, 510

Burrows, A., & Volobuyev, M. 2003, ApJ, 583, 985

Burrows, A., Marley, M. S., & Sharp, C. M. 2000, ApJ, 531, 438

Burrows, A., Hubbard, W. B., Lunine, J. I., & Liebert, J. 2001, Rev. Mod. Phys., 73, 719

Camacho, J. J., Poyato, J. M. L., Pardo, A., & Reyman, D. 1998, J. Chem. Phys., 109, 21

Cohen, J. S., & Schneider, B. 1974, J. Chem. Phys., 61, 3230

Durand, Ph., & Barthelat, J.-C. 1975, Theoret. Chim. Acta, 38, 283

El Hadj Ben Rhouma, M., Berriche, H., Ben Lakhdar, Z., & Spiegelman, F. 2002, J. Chem. Phys., 116, 1839

Foucrault, M., Millié, P., & Daudey, J. P. 1992, J. Chem. Phys., 96, 1257

Geballe, T. R., Saumon, D., Legget, S. K., et al. 2001, ApJ, 556, 373

Huron, B., Malrieu, J. P., & Rancurel, P. 1973, J. Chem. Phys., 58, 5745

Jeung, G. H., Malrieu, J.-P., & Daudey, J.-P. 1982, J. Chem. Phys., 77, 3571

Johnas, C. M. S., Allard, N. F., Homeier, D., Allard, F., & Hauschildt, P. H. 2006, 18th International Conference on Spectral Line Shapes (ICSLS) June 2006, Alabama

Kolos, W., & Wolniewicz, L. 1968, J. Chem. Phys., 49, 404

Liebert, J., Reid, I. N., Burrows, A., et al. 2000, ApJ, 533, L155

Magnier, S., & Millié, Ph. 1996, Phys. Rev. A, 54, 204

Magnier, S., Aubert-Frécon, M., & Allouche, A. R. 2004, J. Chem. Phys., 121, 1771

Marley, M. S., Seager, S., Saumon, D., et al. 2002, ApJ, 568, 335

Müller, W., & Meyer, W. 1984, J. Chem. Phys., 80, 3311

Müller, W., Flesch, J., & Meyer, W. 1984, J. Chem. Phys., 80, 2397

Pascale, J. 1983, Phys. Rev. A, 28, 632

Rafi, M., Al-Tuwirqui, R., & Fayyazuddin 1996, J. Phys.: At. Mol. Opt. Phys. B, 29, L533

Rossi, F., & Pascale, J. 1985, Phys. Rev. A, 32, 2657 (RP85)

Royer, A. 1978, Acta Phys. Pol. A, 54, 805

Santra, R., & Kirby, K. 2005, J. Chem. Phys., 123, 214309 (SK05)

Saumon, D., Geballe, T. R., Leggett, S. K., et al. 2000, ApJ, 117, 1010

Spiegelman, F., Maron, L., Mestdagh, J.-M., Breckenridge, W., & Visticot, J.-P. 2002, J. Chem. Phys., 117, 7534

Spiegelman, F. 2006, to be submitted (S06)

Stwalley, W. C., Zemke, W. T., & Yang, S. C. 1991, Chem. Ref. Data, 20, 153

Szudy, J., & Baylis, W. 1975, J. Quant. Spectrosc. Radiat. Trans., 15, 641

Szudy, J., & Baylis, W. 1996, Phys. Rep., 266, 127

Theodorakopoulos, G., & Petsalakis, I. D. 1993, J. Phys. B., 26, 4367

Tsuji, T., Ohnaka, K., & Aoki, W. 1999, ApJ, 520, L119

Zhu, C., Babb, J. F., Dalgarno, A., 2005, Phys. Rev. A, 71, 052710

Zhu, C., Babb, J. F., Dalgarno, A., 2006, Phys. Rev. A, 73, 012506